Automatica 142 (2022) 110340

Contents lists available at ScienceDirect

Automatica

journal homepage: www.elsevier.com/locate/automatica

Brief paper

Voltage regulation and current sharing for multi-bus DC microgrids: A compromised design approach☆

Handong Bai[a], Hongwei Zhang[b,*], He Cai[c], Johannes Schiffer[d,e]

[a] Key Laboratory of Magnetic Suspension Technology and Maglev Vehicle, Ministry of Education, School of Electrical Engineering, Southwest Jiaotong University, Chengdu, Sichuan 611756, PR China
[b] School of Mechanical Engineering and Automation, Harbin Institute of Technology, Shenzhen, Guangdong 518055, PR China
[c] School of Automation Science and Engineering, South China University of Technology, Guangdong 510641, PR China
[d] Brandenburg University of Technology Cottbus-Senftenberg, 03046 Cottbus, Germany
[e] Fraunhofer Research Institution for Energy Infrastructures and Geothermal Systems (IEG), 03046 Cottbus, Germany

ARTICLE INFO

Article history:
Received 23 November 2020
Received in revised form 16 December 2021
Accepted 16 March 2022
Available online xxxx

Keywords:
Current sharing
DC microgrid
Multi-agent system
Voltage regulation

ABSTRACT

It is well known that accurate current sharing and voltage regulation are both important, yet conflicting control objectives in multi-bus DC microgrids. In this paper a distributed control scheme is proposed, which simultaneously considers these two control objectives via a trade-off factor. This factor permits to adjust the degree of compromise between accurate voltage regulation and current sharing. At the same time, the voltage of a critical node can be precisely regulated. A sufficient condition for closed-loop stability is given and it is shown that the control parameters can always be chosen, such that stability is guaranteed. In addition, the steady state voltage and current deviations relative to their rated values are quantified via suitable metrics. For a given topology and settings of a DC microgrid, a sufficient condition for the existence of the trade-off factor is provided. The results are illustrated by simulation examples.

1. Introduction

The efficient and reliable integration of large shares of distributed generators (DGs) poses significant challenges for the power system operation. To address (part of) these challenges, microgrids have been proposed as a conceptual solution (Lasseter, 2002). A microgrid is a locally controllable system on the distribution or sub-transmission level formed by several DGs, storage units and loads. While the legacy power system is operated with alternating current (AC), the implementation of direct current (DC) systems and in particular DC microgrids can be advantageous in diverse settings, including data centers and industrial production sites (Justo et al., 2013). This has led to an increasing attention on the operation of DC microgrids in both power and control communities in recent years (Cucuzzella et al., 2018; Liu et al., 2018; Maknouninejad et al., 2014; Nahata et al., 2020; Nasirian et al., 2015; Tucci et al., 2018).

In the present paper, we focus on two main control objectives in the operation of DC microgrids, namely voltage regulation and load sharing. Voltage regulation seeks to maintain the bus voltages within a reasonable neighborhood around their rated values. Load sharing means to ensure a fair power allocation amongst DGs. In DC microgrids, the objective of load sharing is often implemented in terms of current sharing (Dragičević et al., 2015). To achieve these objectives, usually a hierarchical control scheme is adopted in DC microgrids (Bidram & Davoudi, 2012). Therein, in the primary control layer mostly the droop control method is employed to realize the coordination of DGs without communication, and a secondary control layer is used to improve the current sharing accuracy and support the stabilization of the bus voltages. In order to avoid a single point of failure caused by centralized control approach, such secondary control schemes are often implemented in a distributed manner (Dragičević et al., 2015; Liu et al., 2018). In this situation, each converter has an independent coordinating controller and a sparse communication network is constructed to exchange information between these controllers. This setup is also adopted in the present work.

Generic meshed DC microgrids with long-distance transmission lines can be modeled by multi-bus DC microgrids, where impedances of the transmission lines cannot be neglected. In multi-bus DC microgrids, voltage regulation and current sharing turn out to be conflicting objectives (Han et al., 2019). In light of

☆ This work was supported by the National Natural Science Foundation of China under Projects 61773322 and 61803160. The material in this paper was not presented at any conference. This paper was recommended for publication in revised form by Associate Editor Francesco Vasca under the direction of Editor Thomas Parisini.

* Corresponding author.
E-mail addresses: hdbai@my.swjtu.edu.cn (H. Bai), hwzhang@hit.edu.cn (H. Zhang), caihe@scut.edu.cn (H. Cai), schiffer@b-tu.de (J. Schiffer).

https://doi.org/10.1016/j.automatica.2022.110340
0005-1098/

this conflict, most available control approaches thus far prioritize accurate current sharing over precise voltage regulation (Han et al., 2018). In Nasirian et al. (2015), a distributed control strategy was proposed to achieve accurate current sharing, and the average voltage of all DGs is observed in a distributed manner and regulated to a rated value. Similar approaches with average voltage regulation are proposed in Tucci et al. (2018) and Cucuzzella et al. (2018). But such strategies do not guarantee admissible voltage deviations between buses, which is undesirable for scenarios when all bus voltages are required to be within normal operating ranges.

Restricting bus voltage deviations is considered jointly with current sharing in Han et al. (2019), where a compromised control approach is proposed. However, the compromise between current sharing and voltage regulation is not quantified and a guidance for design of the control parameters is not explicitly provided. An optimal control method to simultaneously achieve voltage regulation and current sharing is reported in Ding et al. (2018). Yet, the mechanism of interaction between voltage regulation and current sharing is complicated and the relationship between controller parameters and customer demands is not established. In Cucuzzella et al. (2018), a manifold is designed, integrating both objectives of current sharing and voltage regulation. However, the accuracy of current sharing and voltage regulation is difficult to adjust according to the operating demands.

It follows from the above literature review that to date a suitable control law enabling a dedicated compromise between voltage regulation and current sharing is not available. This motivates the present paper, in which the following main contributions are made.

- A distributed control law is proposed that takes both current sharing and voltage regulation into consideration. It features a trade-off factor to effectively adjust the compromised degree of current sharing and voltage regulation. Meanwhile, the voltage of a critical node, such as the node whose load is very sensitive to its operating voltage, can be precisely regulated.
- A sufficient condition for exponential stability of the closed-loop system's equilibrium point is given. In addition, it is shown that there always exists a choice of control parameters that guarantees stability.
- Expressions for the steady state voltage and current deviations are provided via suitable metrics.
- A sufficient condition for the existence of the trade-off factor is provided.

Notations. The identity matrix is denoted by $\mathbf{E}$. The notation 0 denotes zero scalar, vector or matrix with appropriate dimensions. A diagonal matrix is denoted as $diag(g_1, g_2, \ldots, g_n)$ with $g_i \in \mathbb{R}$ being the ith diagonal entry. A matrix $\mathbf{A} = \left[a_{ij}\right] \in \mathbb{R}^{n\times n}$ is said to be nonnegative (positive), denoted by $\mathbf{A} \geq 0$ ($\mathbf{A} > 0$), if $a_{ij} \geq 0$ ($a_{ij} > 0$) for all i, j. The Euclidean norm of a vector $\mathbf{x}$ is denoted by $\|\mathbf{x}\|$. The inner product is denoted by $\langle\cdot,\cdot\rangle$.

2. Preliminaries

2.1. Graph theory

The communication network of a DC microgrid is modeled by a graph $\mathcal{G} = (\mathcal{V}, \mathcal{E})$, where $\mathcal{V} = \{v_1, \ldots, v_N\}$ denotes the set of nodes, i.e. DGs or buses, and $\mathcal{E} \subseteq \mathcal{V} \times \mathcal{V}$ denotes the set of edges, i.e., communication links. The topology of a graph is captured by its adjacency matrix $\mathcal{A} = [a_{ij}] \in \mathbb{R}^{N\times N}$, where a_{ij} is the weight of edge (v_j, v_i), and $a_{ij} > 0$ if $(v_j, v_i) \in \mathcal{E}$; otherwise $a_{ij} = 0$. When $a_{ij} = a_{ji}$, $\forall i, j$, the graph is undirected; otherwise, it is directed. A graph with adjacency matrix $\mathcal{A}$ is denoted as $\mathcal{G}(\mathcal{A})$. The Laplacian matrix $\boldsymbol{\mathcal{L}} = [l_{ij}] \in \mathbb{R}^{N\times N}$ of $\mathcal{G}$ is defined as $l_{ii} = \sum_{j=1}^{N} a_{ij}$ and $l_{ij} = -a_{ij}$ if $i \neq j$. An undirected graph is connected, if there is a path between any two nodes. The adjacency matrix and Laplacian matrix of a connected undirected graph are irreducible (Lewis et al., 2014).

2.2. DC microgrid model

We consider a generic DC microgrid, in which loads are represented by constant impedances.[1] This results in a differential–algebraic system. The algebraic equations can be eliminated via the Kron-reduction method (Bergen & Vittal, 2000). We assume this network reduction has been carried out and consider the Kron-reduced microgrid formed by $N > 1$ nodes.

Following standard practice (Zhao & Dörfler, 2015), we assume that each DG can be represented by a controllable voltage source. Similarly to the case of AC microgrids (Schiffer et al., 2016), this is reasonable if the low-level controls of the converters are sufficiently fast compared to the higher-level controls and the converters can increase and decrease their power output within a certain range. Thus, the DGs are modeled by

$$\mathbf{V} = \mathbf{u},$$

where $\mathbf{V} = [V_1, \ldots, V_N]^T \in \mathbb{R}^N$ is the output voltage of the DG converters, and $\mathbf{u} = [u_1, \ldots, u_N]^T \in \mathbb{R}^N$ is the associated control signal for the converters.

Due to the low operating voltage level of DC microgrids, the impedance of power lines in the system is dominantly resistant. Therefore power lines can be modeled by pure resistances in DC microgrids (Beerten & Belmans, 2013). Then, the power line connecting two nodes i and j in the microgrid is represented by the resistance $R_{ij} > 0$ with associated admittance $Y_{ij} = \frac{1}{R_{ij}}$. If nodes i and j are not directly connected, then $Y_{ij} = 0$. The presence of resistive loads leads to shunt-admittances $\hat{Y}_{ii} = \frac{1}{\hat{R}_{ii}}$, and $\hat{R}_{ii} > 0$ for at least one node in the reduced network. Then, the electrical network of the DC microgrid can be described by the following nodal voltage equation (Bergen & Vittal, 2000)

$$\mathbf{I} = \mathbf{YV} \tag{1}$$

where $\mathbf{I} = [I_1, \ldots, I_N]^{\mathrm{T}} \in \mathbb{R}^N$ denotes the nodal currents and $\mathbf{Y} = \left[y_{ij}\right] \in \mathbb{R}^{N\times N}$ denotes the admittance matrix, where $y_{ii} = \sum_{j\neq i} Y_{ij} + \hat{Y}_{ii}$ and $y_{ij} = -Y_{ij}$.

2.3. Conventional $I - V$ droop control

The primary control of each DG adopts the standard $I - V$ droop control law (Dragičević et al., 2015; Lu et al., 2014), which can be expressed in a compact form as

$$\mathbf{V} = \mathbf{V}^* - \mathbf{\Lambda}\mathbf{I}, \tag{2}$$

where $\mathbf{V}^* = [V_1^*, \ldots, V_N^*]^T$, $\mathbf{\Lambda} = diag(r_1, \ldots, r_N)$, r_i denotes the droop coefficient of the ith DG, and V_i^* denotes the output voltage reference, which can be either a constant or provided by a secondary control law (i.e., a higher-level control). The latter is

[1] Load modeling is a challenging task in power system analysis and there is no uniform load model to characterize all different kinds of loads in a microgrid (Kundur, 1994). This, of course, also applies to the constant impedance load model employed in this paper, which may not accurately represent a dynamic or constant power load over their whole operating range. However, in a neighborhood of an operating voltage, a constant power load can be approximated by a negative resistor, thus resulting in an impedance load (Liu et al., 2018).

the scenario adopted in the present paper. Moreover, the droop coefficients are usually chosen as

$$\mathbf{\Lambda} = \alpha \mathbf{I}^{*^{-1}}, \tag{3}$$

where α is a positive constant, $\mathbf{I}^* = diag(I_1^*, \ldots, I_N^*)$, and I_i^* is the output current rating of the ith DG.

In a DC microgrid described by (1) and (2), accurate current sharing is achieved among DGs, if

$$\frac{I_1}{I_1^*} = \frac{I_2}{I_2^*} = \cdots = \frac{I_N}{I_N^*}. \tag{4}$$

For multi-bus DC microgrids, accurate current sharing will be deteriorated by uncertain resistances between buses (Beerten & Belmans, 2013). To achieve accurate current sharing, an established way is to employ consensus based cooperative control strategies to compensate droop control (Nasirian et al., 2015).

2.4. Relation of current sharing and voltage regulation

For multi-bus DC microgrids, if accurate current sharing is attained, then what is the relation between the DGs' output voltages? The following fact provides an answer, which has an important implication that, under the constraint of accurate current sharing among the DGs, it is impossible to arbitrarily regulate all bus voltages.

Fact 1. *Consider a multi-bus DC microgrid described by (1) and (2). Assume that accurate current sharing is achieved among DGs. If the voltage reference V_i^* of one DG is given, then all nodal voltages and the voltage references of all remaining DGs are uniquely determined.*

3. A control law considering both voltage regulation and current sharing

3.1. Problem formulation

For DC microgrids, there are two typical objectives of voltage regulation: (1) adjust the voltage of a critical node to reach the rated value; (2) restrict deviations between node voltages and their rated values. However, according to Fact 1, when accurate current sharing is achieved and the voltage of the critical node is adjusted to its rated value, voltages of all remaining nodes are determined accordingly. Therefore, to reduce the node voltage deviations, the only way is to sacrifice the accuracy of current sharing, i.e., a trade-off must be made. To formalize these objectives, we introduce the following notions.

Definition 1. The voltage and current deviation ratios for the ith DG are defined respectively as

$$\Delta_i^V = \frac{V_i - V_{rat}}{V_{rat}} \text{ and } \quad \Delta_i^I = \frac{I_i^{pu} - I_{avg}^{pu}}{I_{avg}^{pu}},$$

where V_{rat} is the rated voltage of the DC microgrid, $I_i^{pu} = I_i/I_i^*$ is the per unit current of node i, and $I_{avg}^{pu} = \sum_{i=1}^N I_i^{pu}/N$. Furthermore, the maximum voltage (or current) deviation ratio is $\Delta_{max}^V = \max_i |\Delta_i^V|$ (or $\Delta_{max}^I = \max_i |\Delta_i^I|$), and the average voltage (or current) deviation ratio is $\Delta_{avg}^V = \frac{1}{N}\sum_{i=1}^N |\Delta_i^V|$ (or $\Delta_{avg}^I = \frac{1}{N}\sum_{i=1}^N |\Delta_i^I|$).

These four metrics Δ_{max}^V, Δ_{avg}^V, Δ_{max}^I and Δ_{avg}^I provide measures of the degree of current sharing and voltage regulation of a DC microgrid. We are now in a position to state the problem of interest of this paper.

Problem 1. Consider the system (1) and (2). Given the voltage reference V_{rat} at the kth node, and two positive constants Γ_V and Γ_I, suppose there exist corresponding V_i, $i = 1, \ldots, N$, such that $\Delta_{max}^V \le \Gamma_V$ and $\Delta_{max}^I \le \Gamma_I$. Design a distributed secondary control law for the signal $\mathbf{V}^*$ such that the following three objectives are achieved

$$\lim_{t\to\infty} V_k = V_{rat}, \quad \lim_{t\to\infty} \Delta_{max}^V \le \Gamma_V, \quad \lim_{t\to\infty} \Delta_{max}^I \le \Gamma_I.$$

3.2. Control law design

To solve Problem 1, we propose the following distributed control law for V_i^* in (2) as

$$V_i^* = \phi_i + \theta V_i \tag{5a}$$

$$\dot{\phi}_i = \sum_{j=1}^N a_{ij}\left(\phi_j - \phi_i\right) + g_i\left(V_{rat} - V_i\right). \tag{5b}$$

where $a_{ij} \ge 0$ are the elements of the adjacency matrix $\mathcal{A}$ of the communication graph $\mathcal{G}(\mathcal{A})$, and g_i denotes the weight of the edge from the virtual leader (i.e., V_{rat}) to the ith node, with $g_i > 0$ if node v_i is the critical node; otherwise $g_i = 0$. The design parameter $\theta \in [0, 1]$ is a trade-off factor to adjust the degree of current sharing and voltage regulation of DGs. When $\theta = 0$ (or $\theta = 1$), accurate voltage regulation (or current sharing) will be achieved. By picking $\theta \in (0, 1)$, both current sharing and voltage regulation will be taken into consideration simultaneously, and the weights of these two control objectives can be easily adjusted by θ.

Fact 1 implies that it is generally impossible to regulate the voltage references of two different nodes to an identical rating, when accurate current sharing is required. Thus, we need the following assumption.

Assumption 1. In (5b), $g_i > 0$ for only one $i \in \{1, \ldots, N\}$ and $g_j = 0$ for all $j \ne i$. Moreover, the communication graph $\mathcal{G}(\mathcal{A})$ is undirected and connected.

3.3. Dynamics of the closed-loop system

In this subsection, the dynamics of the closed-loop system of the DC microgrid (1), (2) with the distributed secondary controller (5) are derived.

Let $\mathbf{\Phi} = [\phi_1, \ldots, \phi_N]^T \in \mathbb{R}^N$. Then, considering (1), (2) and (5a), we have

$$\mathbf{\Phi} = \left(\mathbf{\Lambda}\mathbf{Y} + (1-\theta)\,\mathbf{E}\right)\mathbf{V}. \tag{6}$$

If $\theta \in [0, 1]$, then the matrix $\left(\mathbf{E} + (1-\theta)\,\mathbf{Y}^{-1}\mathbf{\Lambda}^{-1}\right)$ is nonsingular (Johnson, 1982, Theorem 3). Thus,

$$\mathbf{V} = \mathbf{N}(\theta)\mathbf{\Phi}, \tag{7}$$

where $\mathbf{N}(\theta) = [n_{ij}] = \mathbf{Y}^{-1}\mathbf{\Lambda}^{-1}\mathbf{H}(\theta)$ and $\mathbf{H}(\theta) = [h_{ij}] = \left(\mathbf{E} + (1-\theta)\,\mathbf{Y}^{-1}\mathbf{\Lambda}^{-1}\right)^{-1}$. Substituting (7) into the compact form of (5b) yields the closed-loop system

$$\dot{\mathbf{\Phi}} = \mathbf{A}_c(\theta)\mathbf{\Phi} + \mathbf{G}\underline{\mathbf{V}}_{rat}, \tag{8}$$

where $\mathbf{A}_c(\theta) = -\left(\boldsymbol{\mathcal{L}} + \mathbf{G}\mathbf{N}(\theta)\right)$, $\underline{\mathbf{V}}_{rat} = V_{rat}\underline{\mathbf{1}}_N = V_{rat}[1, \ldots, 1]^T$, $\mathbf{G} = diag(g_1, \ldots, g_N)$, and $\boldsymbol{\mathcal{L}}$ is the Laplacian matrix of the communication graph.

3.4. Stability analysis

Before analyzing stability of the closed-loop system, we first establish some preliminary results.

Lemma 1. *Let* $\mathbf{A} \in \mathbb{R}^{N\times N}$ *be a nonsingular* $\mathcal{M}$*-matrix and irreducible. Let* $\mathbf{D}$ *be a positive diagonal matrix. Then* $(\mathbf{A}+\alpha_1\mathbf{D})^{-1} > (\mathbf{A}+\alpha_2\mathbf{D})^{-1},\ \forall\alpha_2 > \alpha_1 > 0$.

Lemma 2. *Matrix* $\mathbf{N}(\theta)$ *is an inverse* $\mathcal{M}$*-matrix, for all* $\theta \in [0, 1]$*. Let* $\theta_1, \theta_2 \in [0, 1]$ *and* $\theta_1 < \theta_2$*. Then we have* $0 < (\mathbf{\Lambda Y} + \mathbf{E})^{-1} \le \mathbf{N}(\theta_1) < \mathbf{N}(\theta_2) \le \mathbf{Y}^{-1}\mathbf{\Lambda}^{-1}$.

Lemma 3. *Suppose Assumption 1 holds and k is the unique critical node, i.e.,* $g_k > 0$ *and* $g_i = 0$, $\forall i \ne k$*. Then the matrix* $\mathbf{A}_c(\theta)$ *in (8) is nonsingular for any* $\theta \in [0, 1]$.

Now we are ready to present one of our main results which characterizes the steady state solution of system (8) and provides a sufficient condition for its stability.

Theorem 1. *Fix* $\theta \in [0, 1]$*, a constant* $V_{rat} > 0$ *and a critical node* $k \in \{1, 2, \dots, N\}$*. Suppose Assumption 1 holds and*

$$\lambda_2 > \sqrt{\frac{\|\mathbf{n}_k\|^2\left(N\|\mathbf{n}_k\| - \sum_{i=1}^N n_{ki}\right)}{4\sum_{i=1}^N n_{ki}}}, \tag{9}$$

where λ_2 *is the second smallest eigenvalue of* $\boldsymbol{\mathcal{L}}$*, and* $\mathbf{n}_k = [n_{k1}, \dots, n_{kN}]^T$*. Then,*

1. *The system matrix* $\mathbf{A}_c(\theta)$ *of (8) is Hurwitz.*
2. *The virtual voltages* ϕ_i *achieve consensus, i.e.,*

$$\lim_{t\to\infty}\phi_i = \frac{V_{rat}}{\sum_{j=1}^N n_{kj}}, \quad \forall i = 1, \dots, N.$$

3. *The voltage of the critical node k is regulated to the voltage reference, i.e.,* $\lim_{t\to\infty} V_k = V_{rat}$.

Proof. Part (1): According to Lemma 2, we have $\mathbf{n}_k > 0$. With Assumption 1, matrix $\mathbf{GN}$ can be put as $\mathbf{GN} = \mathbf{e}_k\mathbf{n}_k^T$, where $\mathbf{e}_k$ is defined in the proof of Lemma 3 in Appendix. Since $\mathcal{G}$ is undirected and connected, its Laplacian matrix $\boldsymbol{\mathcal{L}}$ has a simple zero eigenvalue with an associated eigenvector $\underline{\mathbf{1}}_N$ (Lewis et al., 2014) and all its other eigenvalues are positive and real, and $\boldsymbol{\mathcal{L}}$ is a singular symmetric $\mathcal{M}$-matrix (Bierkens & Ran, 2014). Moreover, $\mathbf{e}_k$ is not parallel to $\underline{\mathbf{1}}_N$, and $(\underline{\mathbf{1}}_N^T\mathbf{e}_k)(\mathbf{n}_k^T\underline{\mathbf{1}}_N) = \sum_{i=1}^N n_{ki} \ne 0$. Then, according to Theorem 2.7 in Bierkens and Ran (2014), $\mathbf{A}_c$ is Hurwitz if the following inequality holds,

$$\frac{\|\mathbf{e}_k\|\|\mathbf{n}_k\|}{2} < \lambda_2\sqrt{\frac{\beta}{1-\beta}}, \tag{10}$$

where $\beta = \frac{|\langle \mathbf{e}_k, \underline{\mathbf{1}}_N\rangle\langle \mathbf{n}_k, \underline{\mathbf{1}}_N\rangle|}{\|\mathbf{e}_k\|\|\mathbf{n}_k\|\|\underline{\mathbf{1}}_N\|^2}$. By straightforward computation, the inequality (10) can be rewritten as (9).

Part (2): Since $\mathbf{A}_c(\theta)$ is nonsingular (see Lemma 3), we can define $\mathbf{V}_x = \mathbf{\Phi} + \mathbf{A}_c(\theta)^{-1}\mathbf{G}\underline{\mathbf{V}}_{rat}$, which transforms the closed-loop system (8) into the following form

$$\dot{\mathbf{V}}_x = \mathbf{A}_c(\theta)\mathbf{V}_x. \tag{11}$$

Since $\mathbf{A}_c(\theta)$ is Hurwitz, (11) implies that

$$\lim_{t\to\infty}\mathbf{\Phi} = (\boldsymbol{\mathcal{L}} + \mathbf{GN}(\theta))^{-1}\mathbf{G}\underline{\mathbf{V}}_{rat}.$$

Considering $(\boldsymbol{\mathcal{L}} + \mathbf{GN}(\theta))(\boldsymbol{\mathcal{L}} + \mathbf{GN}(\theta))^{-1} = \mathbf{E}$ and letting $(\boldsymbol{\mathcal{L}} + \mathbf{GN}(\theta))^{-1} = [b_{ij}] \in \mathbb{R}^{N\times N}$, we have

$$\begin{cases} \sum_{j=1}^N a_{ij}\left(b_{ik} - b_{jk}\right) = 0, \quad i \in \{1, \dots, N; i \ne k\} \\ \sum_{j=1}^N a_{kj}\left(b_{kk} - b_{jk}\right) + \sum_{j=1}^N b_{jk}n_{kj} = 1. \end{cases} \tag{12}$$

Since the graph $\mathcal{G}(\mathcal{A})$ is undirected and connected, there must exist at least one nonzero element in each row of the adjacency matrix $\mathcal{A}$. Meanwhile, it is important to note that $\mathbf{N}(\theta)$ is independent of the communication graph, and thus a_{ij} is independent of b_{ij}. To satisfy (12), we must have $b_{1k} = \cdots = b_{Nk} = \frac{1}{\sum_{j=1}^N n_{kj}}$. Thus, we have

$$\lim_{t\to\infty}\mathbf{\Phi} = \gamma\underline{\mathbf{1}}_N \tag{13}$$

where $\gamma = V_{rat}/\sum_{j=1}^N n_{kj}$.

Part (3): When steady state is reached, i.e., $\dot{\mathbf{\Phi}} = 0$, considering (7), (8) and (13), we have

$$-\gamma\boldsymbol{\mathcal{L}}\underline{\mathbf{1}}_N + \mathbf{G}\left(\underline{\mathbf{V}}_{rat} - \mathbf{V}\right) = 0. \tag{14}$$

Since $\boldsymbol{\mathcal{L}}\underline{\mathbf{1}}_N = 0$ (Lewis et al., 2014) and only g_k of $\mathbf{G}$ is nonzero, (14) implies $V_k = V_{rat}$ where k is index of the critical node. This completes the proof. □

Theorem 1 provides a sufficient condition (9) for the stability of the closed-loop system. More specifically, (9) implies that for a given DC microgrid, the stability of (8) can be guaranteed by an appropriate design of the communication network. The following corollary shows that this condition can be guaranteed by tuning the design parameter α of the droop controller (2), (3).

Corollary 1. *Fix* $\theta \in [0, 1]$*, a constant* $V_{rat} > 0$ *and a critical node* $k \in \{1, 2, \dots, N\}$*. Under Assumption 1, there exists an* $\alpha_0 > 0$ *such that the equilibrium point of the closed-loop system (8) is exponentially stable for* $\alpha \in (\alpha_0, +\infty)$.

Corollary 2. *Consider the closed-loop system (8). Suppose Assumption 1 and condition (9) hold. Then*

(1) when $\theta = 1$*, accurate current sharing is achieved.*
(2) when $\theta = 0$*, voltage references achieve consensus, i.e.,* $\lim_{t\to\infty}(V_i^* - V_j^*) = 0, \quad \forall i \ne j$.

The proof of Corollary 2 is trivial and thus omitted.

Remark 1. According to Corollary 2, distributed current sharing control laws such as those in Liu et al. (2018), Nasirian et al. (2015), can be regarded as special cases of the controller proposed in this paper.

3.5. Existence of θ for prescribed Γ_V and Γ_I

The performance indices Γ_V and Γ_I given in Problem 1 are provided by consumers or operators. Given Γ_V and Γ_I, the range of the trade-off design parameter θ can be obtained by solving the following set of inequalities

$$\begin{cases} \Delta_{max}^V(\theta) \le \Gamma_V, \\ \Delta_{max}^I(\theta) \le \Gamma_I. \end{cases} \tag{15}$$

Before proceeding, we shall show that the steady state voltage and current deviation ratios can be characterized via $\mathbf{N}(\theta)$ and $\mathbf{H}(\theta)$. This is subsequently used to compute the maximum voltage deviation ratio $\Delta_{max}^V(\theta)$ and the maximum current deviation ratio $\Delta_{max}^I(\theta)$.

Proposition 1. *Consider the closed-loop system (8) with Assumption 1. Fix* $\theta \in [0, 1]$ *and a constant* $V_{rat} > 0$*. Then, in steady state,*

$$\Delta_i^V(\theta) = \frac{\sum_{j=1}^N n_{ij} - \sum_{j=1}^N n_{kj}}{\sum_{j=1}^N n_{kj}},$$

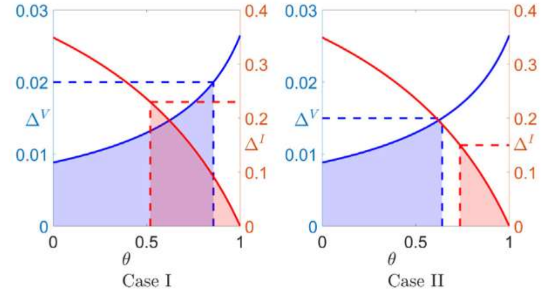

Fig. 1. Solution of θ of Example 1.

$$\Delta_i^I(\theta) = \frac{N\sum_{j=1}^N h_{ij} - \sum_{k=1}^N \sum_{j=1}^N h_{kj}}{\sum_{k=1}^N \sum_{j=1}^N h_{kj}},$$

where k is the index of the critical node.

Now we show through an example, for a reasonable pair of Γ_V and Γ_I, how to choose a proper trade-off parameter θ. In addition, we show that an injudicious choice of Γ_V and Γ_I might lead to an unsolvable problem.

Example 1. Consider the DC microgrid shown in Fig. 2, whose parameters and settings are shown in Section 4. Let node 4 be the critical node. This example aims to find θ for two cases, i.e., Case 1: $\Gamma_V = 0.02$, $\Gamma_I = 0.23$; Case 2: $\Gamma_V = 0.015$, $\Gamma_I = 0.15$. For this given DC microgrid, we first derive $\mathbf{Y}$ and $\mathbf{\Lambda}$ and let $\alpha = 25$. For Case 1, solving $\Delta_{max}^V(\theta) = 0.02$ and $\Delta_{max}^I(\theta) = 0.23$ yields $\theta_d^V = 0.857$, $\theta_d^I = 0.519$. Fig. 1 shows that the reasonable range of θ is $(0.519, 0.857)$. Moreover, Fig. 1 further implies that a larger θ will bring better accuracy of current sharing, while still meets the requirement of voltage deviation; and vise versa. By tuning θ, we can easily get a compromised control of both current sharing and voltage regulation. For Case 2, solving $\Delta_{max}^V(\theta) = 0.015$ and $\Delta_{max}^I(\theta) = 0.15$ yields $\theta_d^V = 0.6409$, $\theta_d^I = 0.7368$. Fig. 1 shows that θ does not exist for Case 2, which means that these two performance indices conflict for the given DC microgrid.

Now a question naturally arises. For a given DC microgrid, how to pick a feasible pair of Γ_V and Γ_I, such that there exists a corresponding θ satisfying (15)? The following theorem provides an answer.

Theorem 2. *Consider the system (1), (2) with the controller (5). The set of inequalities (15) is solvable if*

$$\Gamma_V > \max\{f_1(\Gamma_I), f_2(\Gamma_I)\} \quad (16)$$

where $f_1(\Gamma_I) = \|\eta\,(1+\Gamma_I)\,\mathbf{Y}^{-1}\mathbf{\Lambda}^{-1} - \mathbf{E}\|_\infty$, $f_2(\Gamma_I) = \|\eta\,(1-\Gamma_I)\,\mathbf{Y}^{-1}\mathbf{\Lambda}^{-1} - \mathbf{E}\|_\infty$, *and* $\eta = \max_\theta \left\{ \frac{\underline{\mathbf{1}}_N^T \mathbf{H} \underline{\mathbf{1}}_N}{N\sum_{j=1}^N n_{kj}} \right\}$.

Proof. For a given Γ_I, the inequality $\Delta_{max}^I(\theta) \le \Gamma_I$ is equivalent to $-\Gamma_I \underline{\mathbf{1}}_N \le \mathbf{\Delta}^I \le \Gamma_I \underline{\mathbf{1}}_N$, where $\mathbf{\Delta}^I = [\Delta_1^I, \ldots, \Delta_N^I]^T$. This implies that

$$\bar{I}_{avg}^{pu}(1-\Gamma_I)\underline{\mathbf{1}}_N \le \bar{\mathbf{I}}^{pu} \le \bar{I}_{avg}^{pu}(1+\Gamma_I)\underline{\mathbf{1}}_N,$$

where $\bar{\mathbf{I}}^{pu}$ and $\bar{I}_{avg}^{pu}$ are defined in the proof of Proposition 1 in Appendix. Since $\bar{I}_{avg}^{pu} = \frac{V_{rat}}{\alpha N \sum_{j=1}^N n_{kj}} \underline{\mathbf{1}}_N^T \mathbf{H} \underline{\mathbf{1}}_N$ and $\bar{\mathbf{V}} = \alpha \mathbf{Y}^{-1}\mathbf{\Lambda}^{-1}\bar{\mathbf{I}}^{pu}$, a straightforward computation yields

$$\xi(1-\Gamma_I)\mathbf{Y}^{-1}\mathbf{\Lambda}^{-1}\underline{\mathbf{V}}_{rat} \le \bar{\mathbf{V}} \le \xi(1+\Gamma_I)\mathbf{Y}^{-1}\mathbf{\Lambda}^{-1}\underline{\mathbf{V}}_{rat}$$

where $\xi(\theta) = \frac{\underline{\mathbf{1}}_N^T \mathbf{H} \underline{\mathbf{1}}_N}{N\sum_{j=1}^N n_{kj}}$. It further implies that

$$\xi(1-\Gamma_I)\mathbf{Y}^{-1}\mathbf{\Lambda}^{-1}\underline{\mathbf{1}}_N \le \mathbf{\Delta}^V + \underline{\mathbf{1}}_N \le \xi(1+\Gamma_I)\mathbf{Y}^{-1}\mathbf{\Lambda}^{-1}\underline{\mathbf{1}}_N.$$

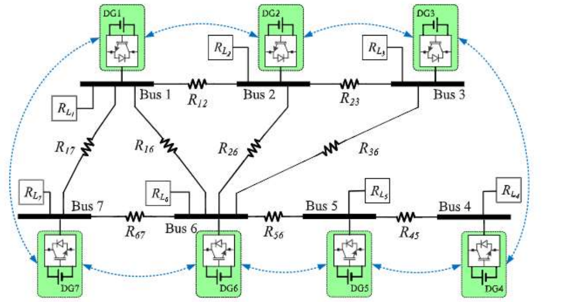

Fig. 2. DC microgrid with 7 buses.

Thus $\Delta_{max}^V \le \max\{f_1(\Gamma_I), f_2(\Gamma_I)\}$. Therefore, a sufficient condition for the existence of θ is (16). □

Theorem 2 justifies the assumption in Problem 1. Now the solvability of Problem 1 is obtained by Theorem 1, Corollary 2 and Theorem 2.

4. Simulation examples

Consider a DC microgrid consisting of 7 DGs (see Fig. 2). The communication network among the DGs is shown by blue dashed lines. Let the weight of each communication link be 1 for simplicity, while bearing in mind that same results hold for general link weights. Let $\mathbf{I}^* = diag(30, 30, 20, 20, 40, 40, 40)$ and $\alpha = 45$. The parameters of loads and transmission lines are: $R_{L_1} = 50\ \Omega$, $R_{L_2} = 20\ \Omega$, $R_{L_3} = 26\ \Omega$, $R_{L_4} = 35\ \Omega$, $R_{L_5} = 38\ \Omega$, $R_{L_6} = 23\ \Omega$, $R_{L_7} = 40\ \Omega$, $R_{12} = 1\ \Omega$, $R_{16} = 1\ \Omega$, $R_{17} = 1\ \Omega$, $R_{23} = 1.2\ \Omega$, $R_{26} = 1\ \Omega$, $R_{36} = 2\ \Omega$, $R_{45} = 1\ \Omega$, $R_{56} = 2\ \Omega$, and $R_{67} = 1\ \Omega$. The rated voltage of the microgrid is set to $V_{rat} = 380$ V. During the first 0.5s, only the local droop control (2) is applied to each DG. At $t = 0.5$s, the distributed secondary controllers (5) are applied and node 3 is set to be the critical node. Then from $t = 5$ s, the critical node is switched to node 5.

The simulation examples consider three cases, namely $\theta = 1$, $\theta = 0$ and $\theta = 0.5$. As shown in Fig. 3, accurate current sharing is not achieved during the first 0.5s. During $t \in [0.5, 5)$s, voltage of the critical node V_3 gradually reaches the rated value $380V$; and during $t \in [5, 10)$s, voltage of the new critical node V_5 approaches $380V$. From the current sharing point of view, for Case I (see Fig. 3(d)), the output currents of all DGs gradually reach accurate sharing; however, for Case II (see Fig. 3(e)), the output currents of the DGs are not accurately shared, and Case III (see Fig. 3(f)) has better current sharing performance than Case II, but worse than Case I.

The performance indices Δ_{max}^I for Case I, II, and III, are 0, 0.2521, and 0.1652, respectively. Moreover, when node 3 is the critical node, the performance indices Δ_{max}^V for Case I, II, and III are 0.0351, 0.0201, and 0.0245, respectively, and when node 5 is set to be the critical node, the performance indices Δ_{max}^V for Case I, II, and III are 0.0339, 0.0192, and 0.0239, respectively. This means that, from the voltage regulation point of view, Case III (see Fig. 3(c)) is better than Case I (see Fig. 3(a)), and slightly worse than Case II (see Fig. 3(b)).

5. Conclusions

This paper studied the mechanism of interaction between current sharing and voltage regulation in DC microgrids, according to which, a novel control method was proposed which takes into account the degree of compromise of current sharing and voltage consensus, and can precisely regulate the bus voltage of a critical node. To quantify the performance of the microgrid,

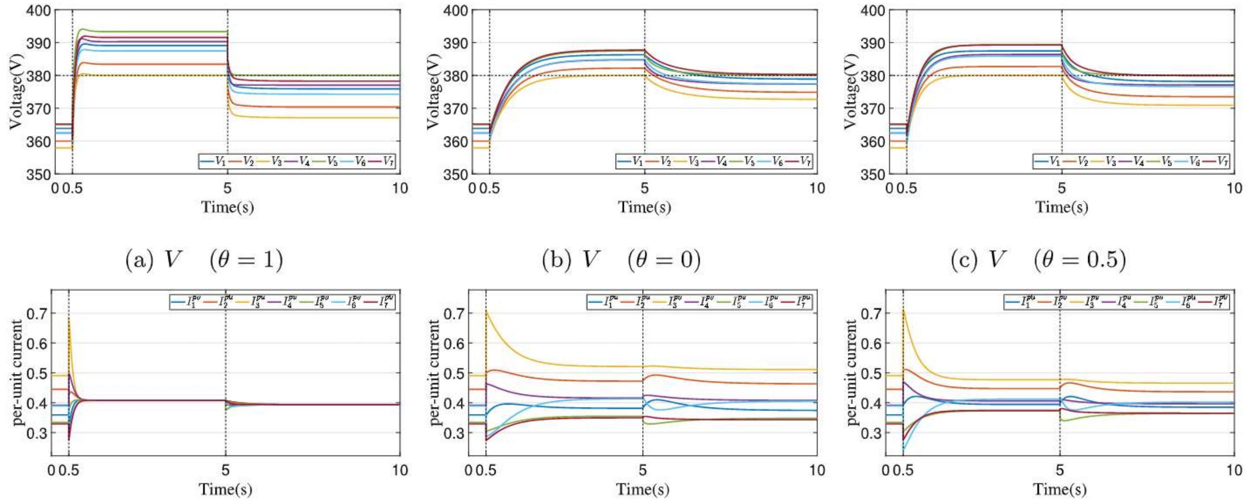

(a) $V \quad (\theta = 1)$ (b) $V \quad (\theta = 0)$ (c) $V \quad (\theta = 0.5)$

(d) $I^{pu} \quad (\theta = 1)$ (e) $I^{pu} \quad (\theta = 0)$ (f) $I^{pu} \quad (\theta = 0.5)$

Fig. 3. The simulation results when $\theta = 0$, 1, and 0.5.

we defined two performance indices, i.e., voltage and current deviation ratios. Moreover, the existence of the trade-off factor is illustrated by an example, and a sufficient condition on consumer specified performance indices Γ_V and Γ_I is provided to guarantee the existence of the trade-off factor θ. For a reasonable pair of Γ_V and Γ_I, how to practically design θ without using any information of the electrical network will be our future work. Also, we plan to investigate robustness of the proposed control scheme with respect to load and parameter uncertainties, and to extend the proposed control scheme to the problem of power, instead of current, sharing.

Appendix

Proof of Fact 1. If all DGs reach accurate current sharing, considering (1) and (4), we have $c\underline{\mathbf{1}}_N = \mathbf{\Lambda}\mathbf{Y}\mathbf{V}$, where $\underline{\mathbf{1}}_N = [1, \ldots, 1]^T \in \mathbb{R}^N$, and c is a positive constant. Since $\mathbf{\Lambda}$ and $\mathbf{Y}$ are invertible (Dörfler et al., 2018), $\mathbf{\Lambda}\mathbf{Y}$ is nonsingular. Considering (2), (3) and (4), we have

$$(\mathbf{\Lambda}\mathbf{Y})^{-1}(\mathbf{\Lambda}\mathbf{Y} + \mathbf{E})\underline{\mathbf{1}}_N = \frac{1}{c}\mathbf{V}^*. \quad (17)$$

Clearly, if one entry V_i^* is fixed, c is uniquely determined. The remaining entries of $\mathbf{V}^*$ then result uniquely from (17) and the corresponding $\mathbf{V}$ is obtained uniquely.

Proof of Lemma 1. Matrices $\mathbf{A} + \alpha_i\mathbf{D}$, $\forall i \in \{1, 2\}$, are still nonsingular $\mathcal{M}$-matrices and irreducible. Then $(\mathbf{A} + \alpha_i\mathbf{D})^{-1} > 0$ (Berman & Plemmons, 1994). It can be shown that

$$(\mathbf{A} + \alpha_1\mathbf{D})^{-1} - (\mathbf{A} + \alpha_2\mathbf{D})^{-1}$$
$$= (\alpha_2 - \alpha_1)(\mathbf{A} + \alpha_1\mathbf{D})^{-1}\mathbf{D}(\mathbf{A} + \alpha_2\mathbf{D})^{-1} > 0.$$

Proof of Lemma 2. Matrix $\mathbf{N}(\theta)$ can be put as

$$\mathbf{N}(\theta) = (\mathbf{\Lambda}\mathbf{Y} + (1 - \theta)\,\mathbf{E})^{-1}. \quad (18)$$

Since $\mathbf{Y}$ is a nonsingular $\mathcal{M}$-matrix (Dörfler et al., 2018), according to Berman and Plemmons (1994), $\mathbf{N}(\theta)^{-1}$ is also a nonsingular $\mathcal{M}$-matrix. Then $\mathbf{N}(\theta)$ is an inverse $\mathcal{M}$-matrix. Noting that $\mathbf{Y}$ is irreducible, from Lemma 1, we have $\left(\mathbf{Y} + (1 - \theta_1)\,\mathbf{\Lambda}^{-1}\right)^{-1} < \left(\mathbf{Y} + (1 - \theta_2)\,\mathbf{\Lambda}^{-1}\right)^{-1}$. Further considering $\mathbf{N}(\theta) = (\mathbf{Y} + (1 - \theta)\,\mathbf{\Lambda}^{-1})^{-1}\,\mathbf{\Lambda}^{-1}$, we can show that $\mathbf{N}(\theta_1) < \mathbf{N}(\theta_2)$. In addition, $\mathbf{N}(0) = (\mathbf{\Lambda}\mathbf{Y} + \mathbf{E})^{-1}$ and $\mathbf{N}(1) = \mathbf{Y}^{-1}\mathbf{\Lambda}^{-1}$. Since $(\mathbf{Y} + \mathbf{\Lambda}^{-1})^{-1} > 0$, $\mathbf{N}(0) = (\mathbf{Y} + \mathbf{\Lambda}^{-1})^{-1}\mathbf{\Lambda}^{-1} > 0$. This completes the proof.

Proof of Lemma 3. Suppose $\mathbf{A}_c$ is singular, i.e., there exists a nonzero vector $\mathbf{x}$, such that $\mathbf{A}_c\mathbf{x} = 0$. For simplicity, let $g_k = 1$. Let $\mathbf{e}_k = [e_i] \in \mathbb{R}^N$ with $e_k = 1$ and $e_i = 0, \forall i \neq k$, and $\mathbf{n}_k = [n_{k1}, \ldots, n_{kN}]^T$. Then, $\mathbf{e}_k\mathbf{n}_k^T = \mathbf{G}\mathbf{N}(\theta)$. Considering $\underline{\mathbf{1}}_N^T\boldsymbol{\mathcal{L}} = 0$, we have

$$\underline{\mathbf{1}}_N^T\mathbf{e}_k\mathbf{n}_k^T\mathbf{x} = \underline{\mathbf{1}}_N^T\left(\boldsymbol{\mathcal{L}} + \mathbf{G}\mathbf{N}\right)\mathbf{x} = -\underline{\mathbf{1}}_N^T\mathbf{A}_c\mathbf{x} = 0. \quad (19)$$

Since $\underline{\mathbf{1}}_N^T\mathbf{e}_k = 1$, (19) implies that $\mathbf{n}_k^T\mathbf{x} = 0$. Moreover, $\boldsymbol{\mathcal{L}}\mathbf{x} = \left(\boldsymbol{\mathcal{L}} + \mathbf{e}_k\mathbf{n}_k^T\right)\mathbf{x} = (\boldsymbol{\mathcal{L}} + \mathbf{G}\mathbf{N})\,\mathbf{x} = -\mathbf{A}_c\mathbf{x} = 0$. According to Lewis et al. (2014), this implies $\mathbf{x} = \eta\underline{\mathbf{1}}_N$, $\eta \in \mathbb{R}$. Further considering the fact that $\mathbf{N} > 0$ (see Lemma 2), we have $\mathbf{x} = 0$. This contradicts with the assumption that $\mathbf{x} \neq 0$. Thus, $\mathbf{A}_c(\theta)$ is nonsingular.

Proof of Corollary 1. Noticing (3), matrix $\mathbf{N}$ in (18) can be further rewritten as $\mathbf{N} = \frac{1}{\alpha}\left(\mathbf{I}^{*-1}\mathbf{Y} + \frac{1-\theta}{\alpha}\mathbf{E}\right)^{-1}$, which tends to zero as $\alpha \to \infty$. Hence, the right hand side of inequality (9) tends to zero. Further, according to the Cauchy–Schwarz inequality, we have $\sum_{i=1}^N n_{kj} \leq \sqrt{N}\|\mathbf{n}_k\| < N\|\mathbf{n}_k\|$, $\forall N > 1$. This implies that the right hand side of the inequality (9) is always positive. Due to the continuity of the right hand side of (9) on α, for a given positive λ_2, there exists an $\alpha_0 > 0$ such that (9) is satisfied for all $\alpha \in (\alpha_0, +\infty)$.

Proof of Proposition 1. Considering (7) and (13), we have the steady state nodal voltage $\bar{\mathbf{V}} = [\bar{V}_i] = \lim_{t\to\infty}\mathbf{V} = \mathbf{N}(\theta)\gamma\underline{\mathbf{1}}_N$. Then

$$\Delta_i^V(\theta) = \frac{\bar{V}_i - V_{rat}}{V_{rat}} = \frac{\sum_{j=1}^N n_{ij} - \sum_{j=1}^N n_{kj}}{\sum_{j=1}^N n_{kj}}.$$

Considering (2), (6) and (13), we have $\bar{\mathbf{I}}^{pu} = [\bar{I}_i^{pu}] = \lim_{t\to\infty}\mathbf{I}^{pu} = \frac{\gamma}{\alpha}\mathbf{H}(\theta)\underline{\mathbf{1}}_N$. Thus $\bar{I}_i^{pu} = \frac{\gamma}{\alpha}\sum_{j=1}^N h_{ij}$. Then straightforward computation yields

$$\Delta_i^I(\theta) = \frac{\bar{I}_i^{pu} - \bar{I}_{avg}^{pu}}{\bar{I}_{avg}^{pu}} = \frac{N\sum_{j=1}^N h_{ij} - \sum_{k=1}^N\sum_{j=1}^N h_{kj}}{\sum_{k=1}^N\sum_{j=1}^N h_{kj}}.$$

References

Beerten, J., & Belmans, R. (2013). Analysis of power sharing and voltage deviations in droop-controlled DC grids. *IEEE Transactions on Power Systems*, *28*(4), 4588–4597.

Bergen, A. R., & Vittal, V. (2000). *Power systems analysis* (2nd ed.). New Jersey: Prentice Hall.

Berman, A., & Plemmons, R. J. (1994). *Nonnegative matrices in the mathematical sciences*. Philadelphia: Society for Industrial and Applied Mathematics.

Bidram, A., & Davoudi, A. (2012). Hierarchical structure of microgrids control system. *IEEE Transactions on Smart Grid*, *3*(4), 1963–1976.

Bierkens, J., & Ran, A. (2014). A singular M-matrix perturbed by a nonnegative rank one matrix has positive principal minors; is it D-stable? *Linear Algebra and Its Applications*, *457*, 191–208.

Cucuzzella, M., Trip, S., De Persis, C., Cheng, X., Ferrara, A., & van der Schaft, A. (2018). A robust consensus algorithm for current sharing and voltage regulation in DC microgrids. *IEEE Transactions on Control Systems Technology*, *27*(4), 1583–1595.

Ding, L., Han, Q., Wang, L., & Sindi, E. (2018). Distributed cooperative optimal control of DC microgrids with communication delays. *IEEE Transactions on Industrial Informatics*, *14*(9), 3924–3935.

Dörfler, F., Simpson-Porco, J. W., & Bullo, F. (2018). Electrical networks and algebraic graph theory: Model, properties, and applications. *Proceedings of the IEEE*, *106*(5), 977–1005.

Dragičević, T., Lu, X., Vasquez, J. C., & Guerrero, J. M. (2015). DC Microgrids - Part I: A review of control strategies and stabilization techniques. *IEEE Transactions on Power Electronics*, *31*(7), 4876–4891.

Han, R., Meng, L., Guerrero, J. M., & Vasquez, J. C. (2018). Distributed nonlinear control with event-triggered communication to achieve current-sharing and voltage regulation in DC microgrids. *IEEE Transactions on Power Electronics*, *33*(7), 6416–6433.

Han, R., Wang, H., Jin, Z., Meng, L., & Guerrero, J. M. (2019). Compromised controller design for current sharing and voltage regulation in DC microgrid. *IEEE Transactions on Power Electronics*, *34*(8), 8045–8061.

Johnson, C. R. (1982). Inverse M-matrices. *Linear Algebra and its Applications*, *47*, 195–216.

Justo, J. J., Mwasilu, F., Lee, J., & Jung, J.-W. (2013). AC microgrids versus DC microgrids with distributed energy resources: A review. *Renewable and Sustainable Energy Reviews*, *24*, 387–405.

Kundur, P. (1994). *Power system stability and control*. New York: McGraw-Hill.

Lasseter, R. H. (2002). Microgrids. In *IEEE power engineering society winter meeting, vol. 1* (pp. 305–308).

Lewis, F. L., Zhang, H., Hengster-Movric, K., & Das, A. (2014). *Cooperative control of multi-agent systems: Optimal and adaptive design approaches*. London: Springer.

Liu, Z., Su, M., Sun, Y., Han, H., Hou, X., & Guerrero, J. M. (2018). Stability analysis of DC microgrids with constant power load under distributed control methods. *Automatica*, *90*, 62–72.

Lu, X., Guerrero, J. M., Sun, K., & Vasquez, J. C. (2014). An improved droop control method for DC microgrids based on low bandwidth communication with DC bus voltage restoration and enhanced current sharing accuracy. *IEEE Transactions on Power Electronics*, *29*(4), 1800–1812.

Maknouninejad, A., Qu, Z., Lewis, F. L., & Davoudi, A. (2014). Optimal, nonlinear, and distributed designs of droop controls for DC microgrids. *IEEE Transactions on Smart Grid*, *5*(5), 2508–2516.

Nahata, P., Soloperto, R., Tucci, M., Martinelli, A., & Ferrari-Trecate, G. (2020). A passivity-based approach to voltage stabilization in DC microgrids with ZIP loads. *Automatica*, *113*, Article 108770.

Nasirian, V., Moayedi, S., Davoudi, A., & Lewis, F. L. (2015). Distributed cooperative control of DC microgrids. *IEEE Transactions on Power Electronics*, *30*(4), 2288–2303.

Schiffer, J., Zonetti, D., Ortega, R., Stankovic, A. M., Sezi, T., & Raisch, J. (2016). A survey on modeling of microgrids: From fundamental physics to phasors and voltage sources. *Automatica*, *74*, 135–150.

Tucci, M., Meng, L., Guerrero, J. M., & Trecate, G. F. (2018). Stable current sharing and voltage balancing in DC microgrids: A consensus-based secondary control layer. *Automatica*, *95*, 1–13.

Zhao, J., & Dörfler, F. (2015). Distributed control and optimization in DC microgrids. *Automatica*, *61*, 18–26.

Handong Bai received his M.S. degree from Xihua University, Sichuan, China, in 2010. He is currently pursuing the Ph.D. degree at Southwest Jiaotong University, Sichuan, China. His research interests include cooperative control of multi-agent systems, and its applications on AC/DC microgrids.

Hongwei Zhang received the Ph.D. degree in mechanical and automation engineering from the Chinese University of Hong Kong in 2010. Subsequently, he held postdoctoral positions at the University of Texas at Arlington and the City University of Hong Kong. He held a professorship at Southwest Jiaotong University from 2012 to 2020, and then joined Harbin Institute of Technology, Shenzhen, China in Nov. 2020 as a Professor. His research interests include cooperative control of multi-agent systems, distributed control of microgrids, and active noise control. He is an Associate Editor of Neurocomputing, and Transactions of the Institute of Measurement and Control.

He Cai received the Ph.D. degree in mechanical and automation engineering from the Chinese University of Hong Kong, Hong Kong, China, in 2014. From 2014 to 2017, he worked as a research fellow with the School of Electrical and Electronic Engineering, Nanyang Technological University, Singapore. Since 2017, he has been a full professor with School of Automation Science and Engineering, South China University of Technology, Guangzhou, China. His research interests involve cooperative control of multiagent systems and its applications in intelligent robots and smart grid.

Johannes Schiffer received the Diploma degree in engineering cybernetics from the University of Stuttgart, Germany, in 2009 and the Ph.D. degree (Dr.-Ing.) in electrical engineering from Technische Universität (TU) Berlin, Germany, in 2015. He currently holds the chair of Control Systems and Network Control Technology at Brandenburgische Technische Universität Cottbus-Senftenberg, Germany and leads the business area Control, Automation and Operation Management at the Fraunhofer Research Institution for Energy Infrastructures and Geothermal Systems (IEG). Prior to that, he has held appointments as Lecturer (Assistant Professor) at the School of Electronic and Electrical Engineering, University of Leeds, U.K. and as Research Associate in the Control Systems Group and at the Chair of Sustainable Electric Networks and Sources of Energy both at TU Berlin. In 2017 he and his co-workers received the Automatica Paper Prize over the years 2014–2016. His current research interests include distributed control and analysis of complex networks with application to microgrids and smart energy systems.